Microstructured Materials

DOI: 10.1002/anie.200806241

Multicompartmental Microcylinders**

*Srijanani Bhaskar, Jonathon Hitt, Sei-Won Laura Chang, and Joerg Lahann**

Motivated by their importance to major biomedical applications, such as drug delivery or medical imaging,[1] multifunctional colloids with a controlled size,[2–6] shape,[6–10] and surface chemistry[10–13] have recently emerged. In some cases, such as phagocytosis of particles by macrophages, the shape of particles appears to be at least as important as their size.[14–16] In some instances, particles with cylindrical shapes would be desirable.[14–16] Beyond control of size and shape, future multifunctional colloids will require highly engineered internal particle architectures, as manifested by the presence of multiple substructures and compartments. In its simplest form, two compartments can be arranged concentrically in a particle, resulting in core/shell architectures in which a shell compartment surrounds a center unit. A large number of multifunctional core/shell particles have been synthesized,[17–20] and some have already shown biomedical utility by releasing two different drugs.[19,21] Beyond core/shell particles,[20] a recently developed process based on electrohydrodynamic co-jetting can yield anisotropic bi- and tricompartmental micro- and nanoparticles with spherical envelopes, where individual compartments are co-located next to each other.[22–25] In such particles, individual compartments may have distinct chemical compositions or can be selectively surface-modified. Although the number, size, and arrangement of individual particle compartments may be controlled in a highly predictable manner, to date their shape has been limited to spheres. Herein, we report a simple, reliable, and scalable process that allows fabrication of multicompartmental particles with defined cylindrical shapes. The process involves the fabrication of multicompartmental microfiber bundles using electrohydrodynamic co-spinning followed by an automated microsectioning step to convert the microfiber bundles into multifunctional microcylinders with well-defined internal architectures. Microcutting establishes a versatile, low-cost, and potentially high-throughput method for the fabrication of rod-shaped particles with controlled sizes, aspect ratios, shapes, and surface chemistries (Figure 1).

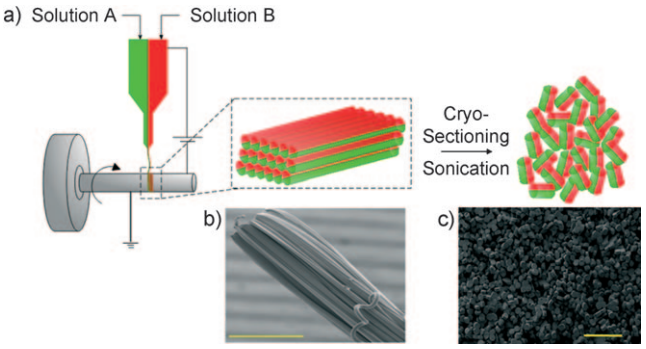

Figure 1. a) The microcutting process, comprised of electrohydrodynamic co-spinning followed by cryosectioning. Two PLGA solutions (A and B, each labeled with a specific fluorophore), are pumped through a side-by-side capillary system under controlled laminar flow. Application of a potential difference to the droplet results in liquid cone formation, droplet stretching and ejection of a fiber, which are deposited onto a spinning wheel assembly that acts as a counter-electrode. The resulting fiber bundles are then subjected to cryosectioning, followed by sonication to yield uniform microcylinders. b) SEM micrograph of bicompartmental fiber bundles obtained by electrohydrodynamic co-spinning (scale bar: 200 μm). c) SEM micrograph of microcylinders prepared by microcutting (scale bar: 100 μm).

Building on recent work that used co-jetting of two or more aqueous polymer solutions to create multicompartmental spheres with diameters in the range of hundreds of nanometers to several microns,[21–25] we turned our attention to electrohydrodynamic co-jetting of poly(lactide-*co*-glycolide) (PLGA) from organic solvents. The major reason for selecting PLGA-based polymers is their biodegradability, which is an important feature for many biomedical applications. A typical electrohydrodynamic co-jetting experiment is shown in Figure 1a. In principle, both multicompartmental particles and fibers can be synthesized in this way; the experimental details that lead to fibers versus particles are described elsewhere.[26] For electrohydrodynamic co-spinning, the jet that ensued from the tip of the cone resulted in the formation of a single fiber, which deposited on the collecting substrate without break-up. Higher PLGA concentrations (18:100 w/w) and low flow rates (between 0.02–0.04 $mL\,h^{-1}$) generally favor the formation of fibers. Incorporation of additional outlet streams enables fabrication of fibers with three or even four compartments,[27] while still maintaining

[*] S. Bhaskar, Prof. J. Lahann
Macromolecular Science and Engineering Program
University of Michigan
Ann Arbor, MI 48109 (USA)
Fax: (+1) 734-764-7453
E-mail: lahann@umich.edu
J. Hitt, S. L. Chang, Prof. J. Lahann
Department of Chemical Engineering, University of Michigan
Ann Arbor, MI 48109 (USA)

[**] *Published on the occasion of the 25th anniversary of the Max Planck Institute for Polymer Research, Mainz.*
We thank Dr. Xuwei Jiang, University of Michigan, for synthesizing the acetylene-functionalized PLGA, Chris Edwards, Microscopy and Image Analysis Lab, University of Michigan, for guidance in cryosectioning, and Prof. David C. Martin, University of Michigan for valuable discussions. J.L. gratefully acknowledges financial support from the Department of Defense (Idea Award, W81XWH-06-1-0271).

Supporting information for this article is available on the WWW under http://dx.doi.org/10.1002/anie.200806241.

the integrity and stability of the jet. This is important, because subsequent processing into microcylinders only becomes feasible if multicompartmental fibers can be deposited as extended bundles of well-aligned microfibers. For this reason, a grounded spinning wheel positioned directly below the needles was used as collecting substrate. By rotation of the wheel assembly (16 rpm), the fiber can be directed to deposit as an ordered bundle for long periods of time (up to 5 h). As this bundle results from continuous deposition of a single fiber, scanning electron microscopy (SEM) images of the bundles revealed near-perfect monodispersity with regard to cylinder diameter within a given bundle (Figure 1b). The simultaneous use of more than two jetting solutions allows the process to be extended to fabrication of tri- and tetraphasic fibers. Similarly, the co-spinning process with three or four outlet streams was extremely stable, could be sustained for several hours, and resulted in tri- and tetra-compartmental microfiber bundles.

Once a reliable process for fabrication of extended bundles of multicompartmental microfibers was established, we elucidated conditions for converting the microfiber bundles into cylindrical particles. A major focus was placed on creating monodisperse microcylinders with definable aspect ratios in an automated or semi-automated process. We ultimately turned to cryosectioning, because it is a straightforward, cost effective strategy for fabricating a variety of well-defined nanostructures of different shapes and sizes.[28] In brief, fiber bundles with an approximate length of 1 cm were harvested, embedded in a gel, and cryosectioned. The cylinder lengths can be conveniently controlled by adjusting the slice thickness and speed of the cryotome to create microcylinders with well-controlled aspect ratios. After dissolution of the embedment gel in water, the particles were suspended in phosphate-buffered saline solution and subjected to pulsed ultrasonication to obtain well-dispersed populations of rod-shaped colloids (Figure 1c). The average diameter of the cylinders is 14 μm and the average length is 5 μm, thus giving an aspect ratio (a.r.) of 0.36. Although the SEM images generally show smooth cylinder surfaces, the edges of cylinders occasionally exhibited some degree of surface roughness along their longitudinal axis, which may be attributed to extensive sonication. Nevertheless, subsequent cross-sectional analysis confirmed the circular character of the multicompartmental microcylinders (Figure 1c and 3b). The quality of cylinders was found to depend on the extent of dryness of the fiber during electrospinning, which, in turn, was found to vary with the different electrospinning process parameters.

An exact positioning of the fiber bundles in the gel matrix normal to the shredding direction is essential for obtaining cylinders with perpendicular vertical and horizontal axes. The overall aspect ratio of the cylinders can be controlled by either tuning the electrospinning process parameters, namely flow rate and electric field strength, thus controlling the diameter, or by assigning a desired length to the microfibers during cryosectioning. Figure 2 shows confocal micrographs of bicompartmental microcylinders of different aspect ratios that were obtained by employing different sectioning intervals during cryosectioning.

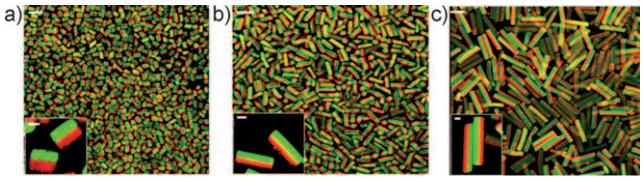

Figure 2. Confocal laser scanning micrographs of bicompartmental microcylinders formed from PLGA and selectively loaded with ADS306PT (red) and PTDPV (green) dyes. By varying the sectioning length, cylinders with different lengths and aspect ratios (a.r.) were prepared: a) length 20 μm, a.r. = 1.3; b) 39 μm, 2.6; c) 80 μm, 4.6. Inlays show high-magnification images. Scale bars: 50 μm for low-magnification images and 10 μm for inlays.

To visualize individual compartments, the microcylinders were characterized by confocal laser scanning microscopy (CLSM). Small amounts of fluorescent polymers (less than 0.1 wt% of polymer in solution) with different spectral emission characteristics (see the Experimental Section) were incorporated into each compartment during co-spinning. After processing, the fluorescent polymers were used to distinguish individual compartments. The compartments shown in Figures 2 and 3a are equally sized and show a well-defined interface, as indicated by a thin line of yellow

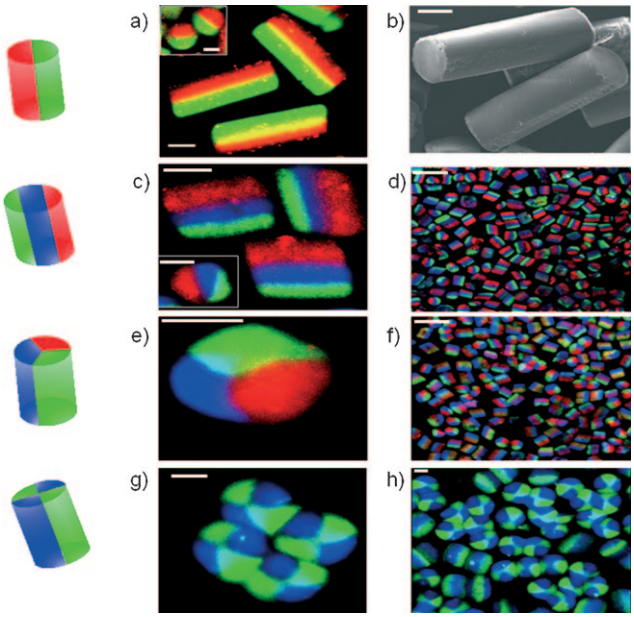

Figure 3. Multicompartmental microcylinders prepared by microcutting. Cartoons indicate the number, nature of fluorescence labeling, and spatial presentation of the individual compartments. a) CLSM image of bicompartmental microcylinders. Inlay shows cross-sectional view. b) Corresponding high magnification SEM image. c,d) High- and low-magnification CLSM micrographs of tricompartmental microcylinders. Inlay in (c) depicts cross-sectional view. e,f) Cross-sectional view and the corresponding low magnification micrograph of pie-shaped microcylinders. g,h) High- and low-magnification CLSM images of rosette-like microcylinders obtained by a square-shaped capillary configuration in which opposite quadrants are loaded with the same dye. Cross-sectional view is shown for better visualization of the individual compartments. Scale bars: d,f) 50 μm; bars in other images are 10 μm.

color between the red and green compartments. (All the cylinders prepared and analyzed in this study were multicompartmental; CLSM images of individual compartments along with the overlays are shown in the Supporting Information, Figure S1). The microcylinders are monodisperse with respect to diameter, the average distribution of the cylinder diameters being within 3 μm, as determined by SEM micrographs (Supporting Information, Figure S2).

An interesting aspect of microcylinders with more than two compartments is that the relative orientation of the compartments emerges as a new design feature; that is, more than one permutation exists as to how three or more equally sized compartments can be arranged. Figure 3c–f show two types of tricompartmental microcylinders. Depending on the initial architecture of the microfibers, cylinders can exist with the blue center compartment sandwiched between two outside red and green compartments (Figure 3c,d). In contrast, a pie-shaped architecture can also be realized (Figure 3e,f). The spatial compartmental orientation is clearly visible in individual fluorescence images and their corresponding overlay (see the Supporting Information, Figure S3). For all the tricompartmental microcylinders, the volume occupied by each phase was almost exactly one third of the entire volume.

Tetracompartmental microcylinders were also produced by loading diagonally opposing nozzles in a square configuration with blue and green fluorophores (Figure 3g,h). This procedure leads to "bow-tie" shapes observed in both the blue and the green fluorescence images, which upon superimposition result in four compartment quadrants. A more pronounced interface (cyan) is observed towards the center, which is the area pulled by the electric field. Again, the phase distribution was identical for all cylinders of a given population, suggesting close to 100% yields. Of note, the distinctive internal architecture of each type of fiber that was produced by co-spinning was well preserved after embedding, sectioning, and sonication into cylinders. Thus, the integration of these two processes may represent a robust platform for future scale-up.

We then proceeded to demonstrate that spatioselective surface modification of multicompartmental microcylinders is possible by employing the Huisgen 1,3-dipolar cycloaddition reaction (Figure 4a).[29–31] For this purpose, microcylinders with "large" and "small" compartments were prepared; that is, tetracompartmental microcylinders with green dye in one phase and blue dye in the other three phases. A small amount of acetylene-functionalized PLGA, poly(lactide-*co*-(propargyl glycolide)),[26,32] was blended into the jetting solution of the smaller compartment, which resulted in the introduction of free acetylene groups into the bulk of the smaller compartment alone; the cone stability was unaltered during co-spinning. We chose a four-compartment cylinder configuration because three fourths of the entire surface area, which was not modified, served as an internal control.

The microcylinders were reacted with biotin-(ethylene oxide)$_3$ azide in the presence of copper sulfate and sodium ascorbate. This resulted in covalent surface immobilization of biotin on one fourth of the cylinder surface. The cylinders were then incubated with streptavidin, which binds to biotin with high selectivity, conjugated with Alexa Fluor 633. Red peripheral fluorescence owing to streptavidin was seen only in one fourth of the lateral surface of the cylinder (Figure 4b), indicating successful selective surface modification. To further substantiate the spatioselectivity, a three-dimensional *z*-stack analysis was performed on a representative cylinder. A series of confocal images was recorded in 1.5 μm increments from top to bottom. The reconstruction of twenty individual slices clearly indicated the presence of green dye adjacent to the red fluorescence from streptavidin throughout the depth of the fiber (Supporting Information, Figure S5). In the three-dimensional CLSM micrographs, the green dye

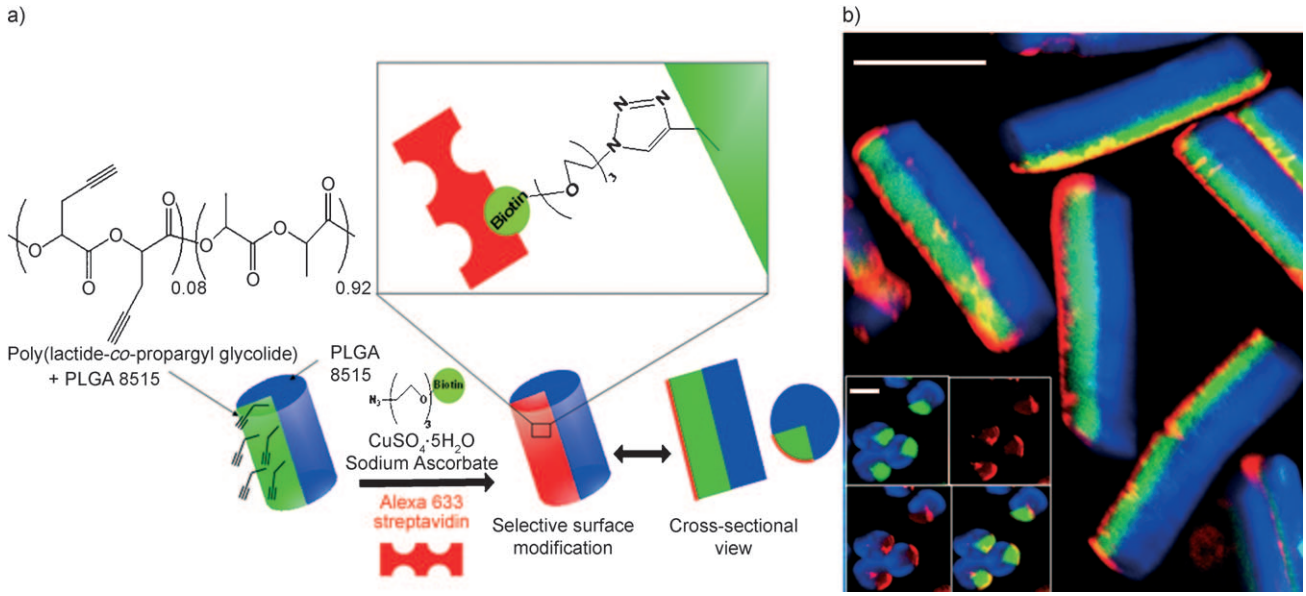

Figure 4. a) Selective surface modification of multicompartmental microcylinders with streptavidin using click chemistry. b) Axial and cross-sectional CLSM micrographs (inset), confirming spatioselective surface modification. Scale bars: 50 μm for the main image, 20 μm for the insets.

present in one fourth of the surface is rendered almost invisible by the red fluorescence from streptavidin, as is seen from front and side views (see also the movie in the Supporting Information). At higher magnifications, a yellow color is seen that is due to overlay of red and green. These results further demonstrate the specificity of the surface modification procedure. Beyond selective surface modification, the microcylinders may contain sacrificial compartments that can be selectively removed, providing access to interesting particle shapes. To demonstrate this idea, we prepared microdisks that were comprised of a three-quarter compartment made of PLGA and a small one-quarter compartment that contained a 63:37 mixture of poly(*N*-isopropyl acrylamide) (PNIPAM) and PLGA. Subsequent exposure to water for several days resulted in indented microdisks formed by selective removal of the PNIPAM compartments (Supporting Information, Figure S6).

In conclusion, we have developed a novel process for fabrication of multifunctional microcylinders and microdisks. Moreover, fabrication of multicompartmental, nearly monodisperse, and biodegradable microcylinders with controllable number, size, and orientation of compartments has been demonstrated. Precise control over aspect ratios is achievable with this technique. The resulting multicompartmental microcylinders with controlled surface patterns may play an important role in the development of next-generation biomaterials with precisely designable physical and chemical properties.[33]

Experimental Section

Electrohydrodynamic co-spinning: Bicompartmental microfibers were fabricated by adapting a previously described method.[26] Two solutions, each 18:100 w/w polymer:solvent and comprised of PLGA (85:15, $M_w = 40$–$75\ kg\,mol^{-1}$, Sigma–Aldrich) in 95:5 v/v chloroform:DMF (Sigma–Aldrich) were prepared. One polymer solution was loaded with trace amounts (< 0.1% w/w polymer) of the red fluorophore ADS306PT (American Dye Source), and the other with the green fluorophore poly[tris(2,5-bis(hexyloxy)-1,4-phenylenevinylene)-*alt*-(1,3-phenylenevinylene)] (PTDPV; Sigma–Aldrich). The polymer solutions were pumped through a side-by-side dual capillary system (Micromedics Inc), which was connected to the cathode of a DC voltage source (Gamma High-Voltage Research). A grounded spinning wheel assembly covered with aluminum foil was used as counter electrode to harvest the fiber bundles. The flow rate was controlled via a syringe pump (kD Scientific) from 0.02–0.04 $mL\,h^{-1}$, and voltage was varied in the range of 7.8–9 kV. For tri- and tetracompartmental fibers, additional capillaries were incorporated in the desired configuration and the blue fluorophore poly[(*m*-phenylenevinylene)-*alt*-(2,5-dibutoxy-*p*-phenylenevinylene)] (MEHPPV; Sigma–Aldrich) was employed in addition to PTDPV and ADS306PT. For selective phase-modification experiments, a 30:70 w/w mixture of poly[lactide-*co*-(propargyl glycolide)]/PLGA was used to prepare the jetting solution at aforementioned concentration.

Cryosectioning and ultrasonication: Microfiber bundles (ca. 3 cm in length) were harvested from the electrospinning wheel and vacuum-dried for 10 h. The bundles were cut into pieces of about 1 cm in length and placed parallel to each other in a rectangular polyethylene cryomold (Sakura Finetec). Optimal cutting temperature (OCT) gel (Sakura Finetec) was added and the mold was frozen at −70 °C for 5 minutes, resulting in a rectangular block of solidified gel with fiber bundles embedded therein. The block was then detached from the mold and sectioned at a rate of about 70 sections per minute using a cryostat microtome (HM550 OMC, Microme) maintained at −20 °C. The sections were harvested in 50 mL centrifuge tubes and allowed to warm to room temperature. The OCT gel was dissolved by washing repeatedly with deionized water. The sections were resuspended in phosphate-buffered saline solution (PBS; pH 7, Sigma–Aldrich) containing 2% v/v Tween-20 (Sigma–Aldrich). The fiber bundles were then separated into individual microcylinders through an ultrasonic processor (Cole–Palmer) delivering 225 W at 20 kHz. Sonication was pulsed, with an interval of 1.5 minutes between successive pulses; the duration of each pulse was 24 s. The time for complete dispersion varied between 15–25 minutes of sonication, depending mainly on number of fibers in the bundles.

Selective surface modification: Microcylinders were suspended in PBS containing 0.01% v/v Tween-20 to a final concentration of 65000 cylinders mL^{-1}. To this suspension, 600 μL of $1\ mg\,mL^{-1}$ aqueous solution of tetrafluorophenylazide-$(EO)_3$-biotin (Pierce Pharmaceuticals, USA) was added, followed by 20 μL of 0.1 M aqueous $CuSO_4{\cdot}5\,H_2O$ and 1.8 mL of 0.1 M sodium ascorbate (Sigma–Aldrich). The reaction mixture was vigorously agitated by magnetic stirring in the dark for 9 h at room temperature. The microcylinders were washed with PBS containing 2% v/v Tween-20 repeatedly by vortexing, centrifugation, and resuspension. The cylinders were then suspended in 2 mL of PBS containing 0.1% v/v Tween-20 and 1% w/v serum bovine albumin (Sigma–Aldrich) and incubated with 4 μL of $1\ \mu g\,\mu L^{-1}$ solution of streptavidin conjugated with Alexa Fluor-633 (Invitrogen) for 2.5 h. The microcylinders were washed repeatedly with 2% Tween-20 in PBS and imaged by CLSM.

Scanning electron microscopy: About 10 μL of an aqueous suspension of microcylinders (1.3×10^6 cylinders mL^{-1}) was placed over a silica surface, and the water was allowed to evaporate at room temperature. The surface was sputtered with gold for 2 min and examined by a scanning electron microscope (Philips XL30 FEG). For size distribution studies, image analysis was performed using Image J software.[34]

CLSM and 3D imaging: About 20 μL of a concentrated aqueous suspension of microcylinders (1.3×10^6 cylinders mL^{-1}) was placed on a glass coverslip and imaged with a confocal laser scanning microscope (Olympus FluoView 500). MEHPPV, PTDPV, ADS306PT, and Alexa Fluor633 were excited by 405 nm UV light, and 488 nm Ar, 533 nm He-Ne green, and 633 nm He-Ne red lasers, respectively. Optical filters of emission wavelength 430–460 nm, 505–525 nm, 560–600 nm, and 660 nm (long pass) were used to visualize the fluorescence of MEHPPV, PTDPV, ADS306PT, and Alexa Fluor 633, respectively. For *z*-stack analysis, the slice thickness was 1.5 μm. Three-dimensional reconstitution and animation were performed using Imaris Bitplane software.

Received: December 21, 2008
Revised: March 11, 2009
Published online: May 15, 2009

Keywords: anisotropy · biodegradable polymers · electrohydrodynamic co-spinning · microparticles · protein immobilization

[1] A. Walther, A. H. E. Müller, *Soft Matter* **2008**, *4*, 663.
[2] K. E. Sung, S. A. Vanapalli, D. Mukhija, H. A. McKay, J. M. Millunchick, M. A. Burns, M. J. Solomon, *J. Am. Chem. Soc.* **2008**, *130*, 1335.
[3] A. S. Utada, E. Lorenceau, D. R. Link, P. D. Kaplan, H. A. Stone, D. A. Weitz, *Science* **2005**, *308*, 537.
[4] S. Q. Xu, Z. H. Nie, M. Seo, P. Lewis, E. Kumacheva, H. A. Stone, P. Garstecki, D. B. Weibel, I. Gitlin, G. M. Whitesides, *Angew. Chem.* **2005**, *117*, 734; *Angew. Chem. Int. Ed.* **2005**, *44*, 724.

[5] C. Berkland, K. Kim, D. W. Pack, *J. Controlled Release* **2001**, *73*, 59.
[6] D. Dendukuri, D. C. Pregibon, J. Collins, T. A. Hatton, P. S. Doyle, *Nat. Mater.* **2006**, *5*, 365.
[7] J. W. Kim, R. J. Larsen, D. A. Weitz, *Adv. Mater.* **2007**, *19*, 2005.
[8] J. P. Rolland, B. W. Maynor, L. E. Euliss, A. E. Exner, G. M. Denison, J. M. DeSimone, *J. Am. Chem. Soc.* **2005**, *127*, 10096.
[9] J. A. Champion, Y. K. Katare, S. Mitragotri, *Proc. Natl. Acad. Sci. USA* **2007**, *104*, 11901.
[10] S. L. Tao, K. Popat, T. A. Desai, *Nat. Protoc.* **2006**, *1*, 3153.
[11] H. Y. Chen, J. M. Rouillard, E. Gulari, J. Lahann, *Proc. Natl. Acad. Sci. USA* **2007**, *104*, 11173.
[12] J. C. Love, B. D. Gates, D. B. Wolfe, K. E. Paul, G. M. Whitesides, *Nano Lett.* **2002**, *2*, 891.
[13] O. Cayre, V. N. Paunov, O. D. Velev, *J. Mater. Chem.* **2003**, *13*, 2445.
[14] J. A. Champion, S. Mitragotri, *Proc. Natl. Acad. Sci. USA* **2006**, *103*, 4930.
[15] S. E. A. Gratton, P. A. Ropp, P. D. Pohlhaus, J. C. Luft, V. J. Madden, M. E. Napier, J. M. DeSimone, *Proc. Natl. Acad. Sci. USA* **2008**, *105*, 11613.
[16] Y. Geng, P. Dalhaimer, S. S. Cai, R. Tsai, M. Tewari, T. Minko, D. E. Discher, *Nat. Nanotechnol.* **2007**, *2*, 249.
[17] F. Caruso, R. A. Caruso, H. Mohwald, *Science* **1998**, *282*, 1111.
[18] D. G. Shchukin, G. B. Sukhorukov, H. Mohwald, *Angew. Chem.* **2003**, *115*, 4610; *Angew. Chem. Int. Ed.* **2003**, *42*, 4472.
[19] S. Sengupta, D. Eavarone, I. Capila, G. Zhao, N. Watson, T. Kiziltepe, R. Sasisekharan, *Nature* **2005**, *436*, 568.
[20] A. Kazemi, J. Lahann, *Small* **2008**, *4*, 1756.
[21] C. Berkland, E. Pollauf, N. Varde, D. W. Pack, K. Kim, *Pharm. Res.* **2007**, *24*, 1007.
[22] K. H. Roh, D. C. Martin, J. Lahann, *Nat. Mater.* **2005**, *4*, 759.
[23] K. H. Roh, D. C. Martin, J. Lahann, *J. Am. Chem. Soc.* **2006**, *128*, 6796.
[24] K. H. Roh, M. Yoshida, J. Lahann, *Langmuir* **2007**, *23*, 5683.
[25] M. Yoshida, K. H. Roh, J. Lahann, *Biomaterials* **2007**, *28*, 2446.
[26] S. Bhaskar, K. H. Roh, X. Jiang, G. L. Baker, J. Lahann, *Macromol. Rapid Commun.* **2008**, *29*, 1655.
[27] S. Bhaskar, J. Lahann, *J. Am. Chem. Soc.* **2009**, DOI: 10.1021/ja900354b.
[28] Q. Xu, R. M. Rioux, G. M. Whitesides, *ACS Nano* **2007**, *1*, 215.
[29] R. Huisgen, *1,3-Dipolar Cycloaddition Chemistry*, Wiley, New York, **1984**.
[30] H. C. Kolb, M. G. Finn, K. B. Sharpless, *Angew. Chem.* **2001**, *113*, 2056; *Angew. Chem. Int. Ed.* **2001**, *40*, 2004.
[31] V. V. Rostovtsev, L. G. Green, V. V. Fokin, K. B. Sharpless, *Angew. Chem.* **2002**, *114*, 2708; *Angew. Chem. Int. Ed.* **2002**, *41*, 2596.
[32] X. Jiang, E. B. Vogel, M. R. Smith III, G. L. Baker, *Macromolecules* **2008**, *41*, 1937.
[33] S. Mitragotri, J. Lahann, *Nat. Mater.* **2009**, *8*, 15.
[34] M. D. Abramoff, P. J. Magelhaes, S. J. Ram, *Biophot. Int.* **2004**, *11*, 36.

